

# On a $Z^0$ signature at next high energy electron-positron colliders.

F. M. L. Almeida Jr., Y. A. Coutinho, J. A. M. Martins Simões,  
A. J. Ramalho and S. Wulck.

Instituto de Física,

Universidade Federal do Rio de Janeiro, RJ, Brazil  
and

M. A. B. do Vale

Universidade Federal de São João del Rei, MG, Brazil

December 24, 2018

## Abstract

The associated production of a  $Z^0$  and a final hard photon in high energy electron-positron colliders is studied. It is shown that the hard photon spectrum contains useful information on the  $Z^0$  properties. This remark suggests that, if a new neutral gauge boson exists for  $M_{Z^0} < \sqrt{s}$ , it will not be necessary to make a new energy run at the  $Z^0$  mass in order to get most of its properties.

PACS 12.60.-i, 14.60.St

---

E-mail: m.almeida@ifurj.br

A general consequence of extended  $SU(3) \times SU(2) \times U(1)$  gauge symmetry is the existence of additional gauge bosons. In the simplest extension one has only a new  $U(1)$  neutral gauge boson  $Z^0$ . This scheme has a natural place in grand unified theories and in some superstring models [1]. In other extended models, like left-right  $SU_L(2) \times SU_R(2) \times U(1)$ , there are new charged and neutral gauge bosons [2]. No experimental confirmation of these hypotheses has been found yet, but it is expected that the next generation of colliders will confirm, or rule out, these models. Following the success of the standard neutral gauge boson  $Z$  discovery, it is also expected that a clear sign of the existence of a  $Z^0$  boson could be found in the resonant production of lepton pairs via  $Z^0 \rightarrow l^+ l^-$  (with  $l = e, \mu, \tau$ ), in next high-energy colliders [3, 4, 5]. These topics have been studied by many authors over the last years [5, 6, 7].

However, in the search for this new neutral gauge boson, there is a major difference with the standard model search for the usual  $Z$ . As the  $Z$  mass was theoretically predicted, colliders were built at the  $Z$  mass energies necessary to study its properties. Since the  $Z^0$  mass is not known, colliders are considered at the highest feasible energy  $\sqrt{s}$ . If indications of a  $Z^0$  signal is found with a mass lower than  $\sqrt{s}$ , a new run near the mass value would be necessary in order to study the  $Z^0$  properties in details. This could be experimentally a very complex, expensive or even an impossible operation. It is important to study alternative methods that could equally well disentangle the  $Z^0$  properties without changing the collider energy.

The purpose of this letter is to present an alternative signature for  $Z^0$  production at the new electron-positron colliders, that could allow us to study its width, decay channels, couplings and so on, at a fixed collider energy  $\sqrt{s} > M_{Z^0}$ . Our main point is the associated production of a  $Z^0$  and a hard photon in the process

$$e^+ e^- \rightarrow Z^0 \gamma : \quad (1)$$

A very simple consequence of the system momentum conservation is that the final high-energy hard photon has an energy given by

$$E_\gamma = \frac{s - (M_{Z^0} - \Delta_{Z^0})^2}{2\sqrt{s}}; \quad (2)$$

where  $\Delta$  and  $\Delta_{Z^0}$  are the fluctuations in the photon energy  $E_\gamma$  and  $Z^0$  mass distributions respectively.

The study of the hard photon energy distribution gives the same information as the direct  $Z^0$  decays, but in a simple and direct way, without the need to obtain the  $Z^0$  mass from its decay products. In order to obtain numerical

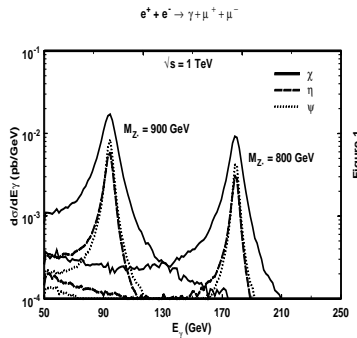


Figure 1

Figure 1: The photon energy distribution in  $e^+ e^- \rightarrow \gamma + \mu^+ + \mu^-$  for  $M_{Z^0} = 800$  GeV and  $M_{Z^0} = 900$  at  $\sqrt{s} = 1$  TeV for the  $\eta$  and  $\eta'$  models. The SM curve is below  $10^{-4}$  pb/GeV.

estimates, detector and hadronization effects, we will employ the canonical  $\eta$  and  $\eta'$  superstring-inspired  $E_6$  models [7], but our arguments apply to any model with extra neutral gauge bosons as well, since it is based on kinematical properties. We neglect  $Z^0 Z^0$  mixing and consider that the  $Z^0$  couples only to usual fermions. Then there is only one unknown parameter in the above models – the extra  $Z^0$  mass.

In order to obtain the hard-photon energy distribution, which is particularly relevant to our analysis, Monte Carlo events were generated and selected by a set of realistic cuts. All final-state particles were required to emerge with a polar angle  $\theta$ , measured with respect to the direction of the electron beam, in the range  $|\cos \theta| > 0.995$ . Events in which the hard-photon energy was less than 50 GeV were ignored. Since we are interested in hard photon emission, this cut eliminates also most of the initial-state radiation. We also imposed a cut  $m_{ij} > 5$  GeV ( $i, j = \gamma, \mu^+, \mu^-$ ) on the invariant masses of the final particles. The  $\cos \theta$  and  $m_{ij}$  cuts reflect roughly the detector limitations. We are assuming that the detector is "blind" for  $|\cos \theta| < 0.995$  and for clusters with  $m_{ij} < 5$  GeV.

As an example of future high energy electron-positron colliders we have chosen the NLC [6, 8] project at an energy  $\sqrt{s} = 1$  TeV and a typical yearly integrated luminosity of  $100 \text{ pb}^{-1}$ .

A first example is given in Fig. 1, which shows the photon energy distribution in the channel  $\gamma + \mu^+ + \mu^-$  for two  $Z^0$  mass values. In order to account for real and virtual contributions for this process we have included all the

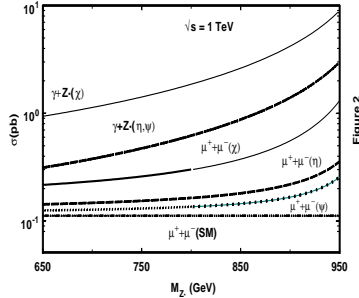


Figure 2: The total cross section for  $e^+ e^- \rightarrow Z^0$  and  $e^+ e^- \rightarrow \gamma^+$  for the  $\chi$ ,  $\eta$ , and standard models.

Models			
Channels			
Hadrons	65;1	79	86
Invisible	16;5	6;9	2;4
$\ell^+ \ell^-$	6;1	4;7	3;9
total = $M_{Z^0}$	0;012	0;005	0;006

Table 1:  $Z^0$  branching ratios (%) and total width for standard fermionic channels in  $\chi$ ,  $\eta$  and standard models.

twelve Feynman diagrams – eight from the standard model and four from the extra  $Z^0$  contribution. We have performed the calculation with the CompHEP package [9]. The corresponding distribution for the SM is below  $10^{-4}$  pb/GeV. A similar distribution, peaked at the photon energy, follows for any other decay channel  $Z^0 \rightarrow \gamma \gamma$ . The  $Z^0$  total cross section is shown in Fig. 2. The cross section for the more usual channel  $e^+ e^- \rightarrow Z^0 \rightarrow \gamma^+$  is also shown for comparison. It is to observe that the  $Z^0$  cross section is greater than  $\gamma^+$  production for all models, including the SM.

In Table 1 we give the  $Z^0$  branching ratios for the fermionic decay channels. For the invisible channel we have summed all neutrinos whereas for the leptonic charged channel individual branching fractions are given. From this result we can estimate the total number of signal events.

With the purpose of accounting for the finite resolution of the NLC de-

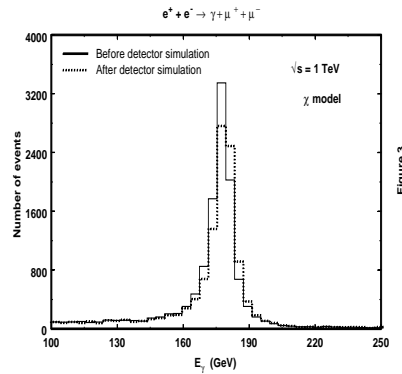


Figure 3: Histogram for the photon energy before and after detector simulation in  $e^+ + e^- \rightarrow \gamma + Z^0 + \mu^+ + \mu^-$  when  $M_{Z^0} = 800$  GeV for  $\chi$  model.

tectors, we smeared the four momenta of the final-state photons and leptons by means of the SM EAR routines [10]. The uncertainties in the energies of the final-state photons were simulated by Gaussian smearing the energies of these particles with a half-width  $E$  of the form  $E = E_0 = a + b = \frac{1}{2}E$ . For the electromagnetic calorimeters proposed for the new linear colliders,  $a = 1\%$  and  $b$  ranges from  $10\%$  to  $15\%$ . We used the value  $b = 12\%$ , which is representative of a NLC electromagnetic calorimeter [8]. The directions of the final-state photons were smeared in a cone around the directions of their original three momenta, according to a Gaussian distribution with half-width equal to  $10\text{ mrad}$ . As far as the detection of muons is concerned, one has to consider the momentum resolution of the muon tracker, and the multiple scattering effects on the transverse momentum  $p_T$  and azimuth of the muons. The details of the procedure to incorporate these effects by Gaussian smearing  $1 = p_T$  and  $\phi$  can be found in Settles et al. [10] and references therein.

The hard photon energy distribution gives a very clear indication of the  $Z^0$  parameters. This is shown in Fig. 3 for the channel  $e^+ + e^- \rightarrow Z^0 + \gamma + \mu^+ + \mu^-$ . The hard photon energy distribution shows practically no difference between the exact theoretical curve and the estimate for the possible data whereas in the reconstructed  $\gamma + Z^0$  invariant mass distribution there is a much larger distortion and the peak shifted to left as shown in Fig. 4. This distortion can lead to experimentally sophisticated invariant mass correction methods increasing the uncertainties for the  $M_{Z^0}$  and its width.

A similar effect can be seen in the hadronic channels. We have performed

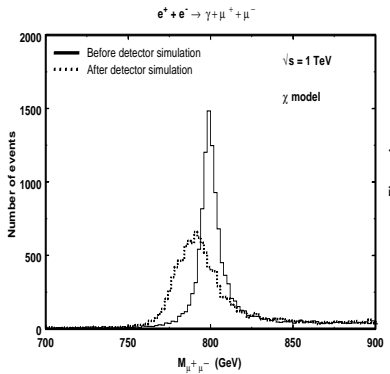


Figure 4

Figure 4: Histogram for the invariant mass before and after detector simulation when  $M_{Z^0} = 800$  GeV for  $\chi$  model.

the full hadronization procedure for the  $Z^0 \rightarrow \gamma \gamma$  by using the Pythia program. The results are shown in Figs. 5-6. Here again the photon peak is practically unchanged, whereas the jet-jet peak presents a much larger distortion. One can also perform the smearing process in the hadronic channels. This will increase even more the distortion in the  $Z^0$  invariant mass reconstruction.

In the hard-photon channel one can also study model differences in the charge forward-backward asymmetry, defined relative to the final angular distribution relative to the incoming electron. The result is shown in Fig. 7.

In conclusion, we have shown that the energy distribution of a hard photon can give a clear indication of a new neutral gauge boson. The asymmetry or/and can be used to distinguish the relevant models. This analysis can be applied to any extended model with an extra neutral gauge boson and to other future high energy lepton colliders.

**Acknowledgments:** This work was partially supported by the following Brazilian agencies: CNPq and FAPERJ.

## References

[1] J. Hewett and T. Rizzo, Phys. Rep. 183 (1989) 193, A. Leike, Phys. Rep. 317, 143 (1999).

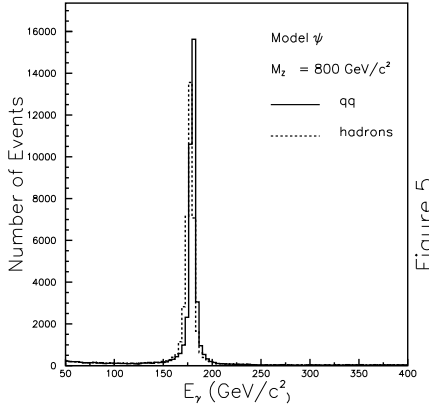


Figure 5

Figure 5: Histogram of the photon energy in jet-jet channel before and after hadronization when  $M_{Z^0} = 800$  GeV for model.

- [2] J.C. Pati and A. Salam, Phys. Rev. D 10 (1974) 275; R.N. Mohapatra and J.C. Pati, Phys. Rev. D 11 (1975) 566; G. Senjanovic and R.N. Mohapatra, Phys. Rev. D 12 (1975) 1502; R.N. Mohapatra and R.E. Marshak, Phys. Lett. B 91 (1980) 222. An extensive list of references can be found in R.N. Mohapatra and P.B. Pal, "Massive Neutrinos in Physics and Astrophysics", World Scientific, Singapore, 1998.
- [3] M. Cvetic and S. Godfrey, hep-ph/9504216; M. Dittmar, A.S.N. Ioillerat and A.D. Jouadi, Phys. Lett. B 583, 111 (2004).
- [4] G. Cvetic and C.S. Kim, Phys. Lett. B 461 (1999) 248 and Phys. Lett. B 471 (2000) 471.
- [5] A.D. Jouadi, J. Ng and T.G. Rizzo in: Electroweak Symmetry Breaking and Beyond the Standard Model. Ed. T. Barklow, S. Dawson, H.E. Haber and S. Siegrist, World Scientific, Singapore. hep-ph/9504210; P. Langacker, M. Luo and A.K. Mann, Rev. Mod. Phys. 64 (1992) 87.
- [6] T. Abe et al. [American Linear Collider Working Group Collaboration], in Proc. of the APS/DPF/DPB Summer Study on the Future of Particle Physics (Snowmass 2001) ed. N. Graf, hep-ex/0106055.
- [7] Particle Data Group, Phys. Lett. B 592 (2004) 1.

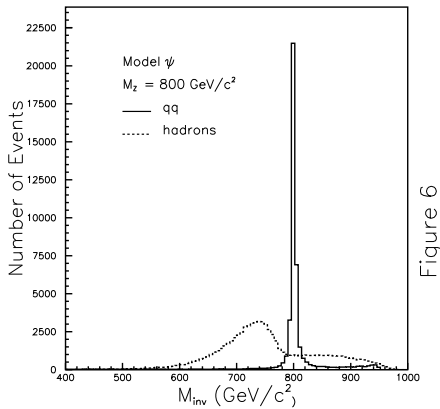


Figure 6

Figure 6: Histogram of the jet-jet invariant mass before and after hadronization when  $M_{Z^0} = 800$  GeV for model.

- [8] S. Kuhlmann et al. [LC ZDR Design Group and LC Physics Working Group Collaboration], [hep-ex/9605011](#).
- [9] A. Pukhov, E. Boos, M. Dubinin, V. Edneral, V. Ilyin, D. Kovalenko, A. Kryukov, V. Savrin, S. Shchannikov and A. Semenov, "Com pHEP" – a package for evaluation of Feynman diagrams and integration over multiparticle phase space. Preprint INP MSU 98-41/542, [hep-ph/9908288](#).
- [10] R. Settles, H. Spiesberger and W. Wienemann, Smear version 3.02; <http://www.desy.de/~hspiesb/smear.html>

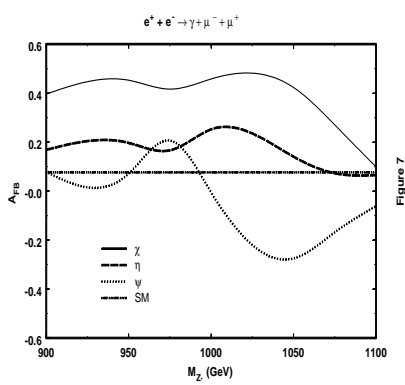


Figure 7

Figure 7: Forward-backward asymmetry as a function of  $M_Z^0$  for the relative to the initial in  $e^+ e^- \rightarrow \gamma + \mu^- + \mu^+$  for the ; and and standard models at  $\bar{p}_s = 1$  TeV .